ORTHOGONAL AND QUASI-ORTHOGONAL TREE CODES WITH APPLICATIONS TO MULTIPLE ACCESS

BY

Dipankar Raychaudhuri & Stephen S. Rappaport

Department of Electrical Engineering
State University of New York
Stony Brook, New York 11794

CEAS REPORT #309

Orthogonal and Quasi-Orthogonal Tree Codes with Applications to Multiple Access

by

Dipankar Raychaudhuri

and

Stephen S. Rappaport

Department of Electrical Engineering
State University of New York
Stony Brook, New York 11794

August 1977

The research reported in this paper was supported in part by the National Science Foundation under grant No. ENG 76-09001.

Orthogonal and Quasi-Orthogonal Tree Codes with Applications to Multiple Access

by

Dipankar Raychaudhuri
and
Stephen S. Rappaport
Department of Electrical Engineering
State University of New York
Stony Brook, New York 11794

Abstract

The performance of orthogonal and quasiorthogonal tree codes is considered for incoherent and coherent systems. In addition several alternative receiver structures using hard quantizing and "greatest-of" detection are treated. Upper bounds on error probability are derived and are used as a basis for system comparison. An application of quasiorthogonal tree codes to a multiple access environment is presented as an example and discussed. Such codes potentially permit reduced bandwidth expansion.

The research reported in this paper was supported in part by the National Science Foundation under grant No. ENG 76-09001.

I. INTRODUCTION:

A. BACKGROUND: Orthogonal tree codes in conjunction with the Viterbi algorithm for maximum likelihood decoding are a feasible alternative to block codes for communication over low signal to noise ratio, power limited channels. Convolutional codes have been treated in detail by Viterbi [1] and the performance of orthogonal tree codes on coherent channels in the presence of white gaussian noise has been considered [3]. In this paper, we consider tree codes using (a) orthogonal signals, and (b) quasi-orthogonal signals. Incoherent and coherent schemes are treated as well as alternative receiver structures using hard quantizing and "greatest of" detection. Upper bounds on error probability are derived and are used as a basis for system comparison. An example application of quasi-orthogonal tree codes in a multiple access environment is discussed.

B. ENCODER & DECODER: Figure 1 shows a convolutional encoder for tree codes. The 2^K signals ($S_k(t)$, k=0,1... 2^K-1) are mutually orthogonal or quasi-orthogonal for orthogonal and quasi-orthogonal tree codes respectively. Each signal has energy E_S; K is the constraint length of the code. With reference to Fig 2, when the signals are orthogonal, it can be observed that any two paths whose generating sequences are not identical over more than K-1 bits at a time, are orthogonal over their entire length. This forms the basis of the decoding algorithm presented by Viterbi [3]. The subsequent analysis assumes an encoder structure as described above and a Viterbi decoder as specified by the algorithm in [3].

C. UPPER BOUND ON ERROR PROBABILITY: An upper bound on the block error probability of a sequence of L bits followed by K-1 synchronizing zeros has been derived in [3], and is obtained by union bounding the probabilities

of error in any comparison which the algorithm makes between two paths. For continuous coherent orthogonal signalling the bound has been shown in [2,3] to be

$$P_E \leq LP_1\left(\frac{SK}{N_0R}\right) + \sum_{k=1}^{L-1} (L-k)\, P_{2^{k-1}}\left[\frac{S}{N_0R}(K+k)\right] \qquad (1)$$

where

$$P_j\left(\frac{SJ}{N_0R}\right) = \text{Prob}\,[z_0 < \max(z_1, z_2 \ldots . z_j)]$$

and $z_0, z_1, \ldots . z_j$ are independent unit variance gaussian random variables, z_0 has mean $\sqrt{2SJ/N_0R}$ and the rest have zero means.

To generalize the above mentioned results to fit any detection scheme, we recognize that z_i is a modified path 'metric' of the i^{th} path under consideration. The term path 'metric' normally means the sum of the optimum branch metrics for all branches on that path. For the continuous coherent case, the optimum branch metric is the inner product of the received signal and the signal corresponding to the branch considered. In general, the optimum branch metric will depend on the actual detection scheme used.

In comparing a correct path with an incorrect adversary, an error will be made when the path metric of the incorrect path exceeds that of the correct one. If the two paths have some branches in common, then the common branch metrics are not relevant to the comparison since they can be cancelled from both path metrics. Cancellation of common terms yields a new metric which can be thought of as the path's 'reduced metric' for that comparison. Because of the nature of the algorithm and bounding argument in [3], each z_i $(i\neq 0)$ encountered in (1) is the reduced metric of path i $(i\neq 0)$ where path i (all $i\neq 0$) differs from the correct path over 'n' branches, and z_0 is the reduced metric of the correct path.

We can now generalize the error probability bound by defining

$$P_{m,n} \triangleq \text{prob}\,[z_0 < \max\,(z_1, z_2 \ldots z_m)] \qquad (2)$$

(m terms)

where $z_1, z_2 \ldots z_m$ are the reduced metrics of 'm' potential adversaries to the correct path, each of which differs from the correct path over the same 'n' branches, and z_0 is the reduced metric of the correct path. Thus, $P_{m,n}$ is the probability that an error will be made in any of 'm' potential comparisons of the correct path to incorrect potential adversaries, each of which differs from the correct path over the same 'n' branches.

The bound can then be expressed as

$$P_E \leq LP_{1,K} + \sum_{k=1}^{L-1} (L-k)\, P_{2^{k-1},\, K+k} \qquad (3)$$

Evaluation of the error probability for tree codes using a given detection scheme therefore requires computation of $P_{m,n}$.

II. EVALUATION OF ERROR PROBABILITY BOUND FOR VARIOUS DETECTION SCHEMES: (IN GAUSSIAN NOISE)

A. INCOHERENT ORTHOGONAL SCHEMES:

1. CONTINUOUS: The receiver structure is shown in Fig. 3. The optimum receiver for low signal to noise ratio, employs a quadratic detector as shown, the output of which is used as the branch metric.

Hence, the reduced path metric z_0 of the correct path is the sum of squares of 'n' independent Rician variates. If A is defined as the signal amplitude at the input to the quadratic detector, z_0 can be written as

$$z_0 = \sum_{i=1}^{n} (A\cos\theta_i + x_i)^2 + \sum_{i=1}^{n} (A\sin\theta_i + y_i)^2 \qquad (4)$$

x_i and y_i are zero mean gaussian random variables with variance σ^2.

The reduced metric for a potential incorrect path is the sum of squares of 'n' statistically independent Rayleigh variates

$$z_i (i \neq 0) = \sum_{j=1}^{n} y_j^2 + \sum_{j=1}^{n} x_j^2 \tag{5}$$

where x_j and y_j are zero mean Gaussian random variables with variance σ^2.

Hence,

$$P_{m,n} = \text{prob}\ [z_0 < \max(z_1, z_2 \ldots z_m)]$$

$$= \int_0^{\infty} \int_{q_1}^{\infty} f_{z_{max}}(q_2)\, dq_2\, f_{z_0}(q_1)\, dq_1 \tag{6}$$

where $z_{max} \triangleq \max(z_1, z_2 \ldots z_m)$ (7)

The reduced metric of the correct path z_0 is statistically independent to the incorrect reduced path metrics $z_i (i \neq 0)$ because they are mutually orthogonal over the 'n' branches. The z_i $(i \neq 0)$ are indentically distributed and statistically independent. Hence

$$f_{z_{max}}(\alpha) = m f_{z_1}(\alpha)\, [F_{z_1}(\alpha)]^{m-1} \tag{8}$$

Since z_0 is the sum of 'n' squared Ricians, it is non-central χ^2 distributed with 2n degrees of freedom and non-centrality parameter nA^2 [4]. The random variable z_1 is χ^2 distributed with '2n' degrees of freedom since it is the sum of squares of 'n' independent Rayleigh variates[4].

Hence, we have,

$$P_{m,n} = \int_0^\infty dq_2 \int_0^\infty dq_1 \, f_{z_0}(q_1) \, f_{z_{max}}(q_2) \tag{9}$$

where,

$$f_{z_0}(\alpha) = \frac{1}{2\sigma^2} \left(\frac{\alpha}{nA^2}\right)^{\frac{n-1}{2}} \exp\left(-\frac{nA^2+\alpha}{2\sigma^2}\right) I_{n-1}\left[\frac{(\alpha nA^2)^{1/2}}{\sigma^2}\right] \tag{10a}$$

$$f_{z_1}(\beta) = \frac{1}{(\sigma^2)^n 2^n \Gamma(n)} \beta^{n-1} \exp\left[-\frac{\beta}{2\sigma^2}\right] \tag{10b}$$

Letting $\xi = \sqrt{q_1}/\sigma$ and $\gamma = \sqrt{n}A/\sigma$

$$\int_0^{q_2} f_{z_0}(\alpha) \, d\alpha = \int_0^{\sqrt{q_2}/\sigma} \xi \left(\frac{\xi}{\gamma}\right)^{n-1} \exp\left(-\frac{1}{2}(\xi^2+\gamma^2)\right) I_{n-1}(\gamma\xi) \, d\xi \tag{11}$$

The above integral can be identified as the complementary generalized Q-function, which is defined in the literature[5] as:

$$Q_M(\alpha,\beta) \triangleq \int_\beta^\infty \xi \left(\frac{\xi}{\alpha}\right)^{M-1} \exp\left[-\frac{1}{2}(\xi^2+\alpha^2)\right] I_{M-1}(\alpha\xi) \, d\xi \tag{12}$$

This yields:

$$P_{m,n} = \int_0^\infty dq_2 \, f_{z_{max}}(q_2) \left\{1-Q_n\left(\frac{\sqrt{n}A}{\sigma}, \frac{\sqrt{q_2}}{\sigma}\right)\right\} \tag{13a}$$

$$= m \int_0^\infty dq_2 \, f_{z_1}(q_2) \left\{F_{z_1}(q_2)\right\}^{m-1} \left\{1-Q_n\left(\frac{\sqrt{n}A}{\sigma}, \frac{\sqrt{q_2}}{\sigma}\right)\right\} \tag{13b}$$

The χ^2 distribution function with k degrees of freedom is defined as[4]

$$G_k(S) = \int_0^S \frac{1}{2^{k/2}\Gamma(k/2)} \alpha^{k/2-1} \exp\left(-\frac{\alpha}{2}\right) d\alpha \tag{14}$$

Therefore, $$F_{z_1}(q_2) \equiv G_{2n}\left(\frac{q_2}{\sigma^2}\right) \tag{15}$$

$$P_{m,n} = m\int_0^\infty dq_2\, f_{z_1}(q_2)\, \{G_{2n}\left(\frac{q_2}{\sigma^2}\right)\}^{m-1}\, \{1-Q_n\left(\frac{\sqrt{n}A}{\sigma}, \frac{\sqrt{q_2}}{\sigma}\right)\} \tag{16a}$$

Letting $y = q_2/\sigma^2$, we obtain

$$P_{m,n} = m\int_0^\infty dy\, \frac{1}{2^n\Gamma(n)}\, y^{n-1} \exp\left(-\frac{y}{2}\right) \{G_{2n}(y)\}^{m-1}\, \{1-Q_n\left(\frac{\sqrt{n}A}{\sigma}, \sqrt{y}\right)\} \tag{16b}$$

Substituting $y = 2x$

$$P_{m,n} = \int_0^\infty dx \exp(-x)\, h(x)$$

where $$h(x) = \frac{x^{n-1}}{\Gamma(n)} \{G_{2n}(2x)\}^{m-1} \{1-Q_n(\sqrt{n}S, \sqrt{2x})\}. m \tag{17}$$

CALCULATION PROCEDURE:

The above integral for $P_{m,n}$ can be evaluated using the Gaussian Laguerre quadrature formula[7,9]. A 10-point integral was used in actual calculation.

The above calculation requires h(x) to be supplied as a function. This necessitates routines for (i) cumulative χ^2 distribution function (ii) generalized complementary Q function. The χ^2 distribution function is available as a subroutine in most computing facilities. The complementary Q function has been variously computed[10,11,5], but a simple and accurate way is to use a Chernoff bounding technique[5]. The formula used is

$$(1-2\lambda)^{-M} \exp(-\lambda\beta^2) \exp(\lambda\alpha^2/(1-2\lambda)) > \begin{cases} Q_M(\alpha,\beta) & ; \beta^2 > \alpha^2 + 2M \\ 1-Q_M(\alpha\beta) & ; \beta^2 < \alpha^2 + 2M \end{cases} \quad (18)$$

The optimum value of λ is given by

$$\lambda_o = 2^{-1}\{1-(M/\beta^2) - (M/\beta^2)[1+(\tfrac{\alpha\beta}{M})^2]^{1/2}\} \quad (19)$$

We use the bound (18) on $1-Q_M(\alpha,\beta)$ where applicable and elsewhere bound $1-Q_M(\alpha,\beta)$ by 1. Thus the evaluated error probability is always an upper bound.

In this manner $P_{m,n}$ is found and P_E is computed from (3). It may be pointed out here that for a data block length of 100 or more 2^{k-1} in the equation can become very large, and make direct evaluation difficult. However since $P_{m,n}$ is given by (17) where $m \equiv 2^{k-1}$ in (3), and $G_{2n}(y)$ is a probability distribution which is less than or equal to one, for large k, $P_{m,n} \to 0$. Moreover the (L-k) multiplying factor in (3) reduces the weight on higher k terms. Physically this would imply that comparison of a very long correct path with an incorrect one produces a very low error probability. In fact, computer results indicate that the $LP_{1,K}$ term in (3) predominates and that the sum giving P_E is determined, usually by the first 5-10 terms.

Example results are shown in Fig.8(a) for a block length L=200 and K from 3-7, and in Fig. 8(b) for K=5 and varying L. These will be discussed in detail subsequently.

2. HARD QUANTIZING (ORTHOGONAL)

Nest we consider an incoherent receiver (Fig. 4) with a hard quantized output which serves as the branch metric for the decoding algorithm. In particular, the decoder now receives zero and one instead of a continuum

of values. The analysis of this case becomes simpler since the reduced path metrics are now binomially distributed.

As before:

$$P_{m,n} = \text{prob}(z_0 < \max(z_1, z_2 \ldots z_m)) \text{ for paths differing over n branches}$$

where

z_0: reduced metric of correct path

$z_i (i \neq 0)$: reduced metrics of potential incorrect adversaries.

Since z_0 is the sum of 'n' branch metrics which are either 0 or 1, with probabilities q and (1-q) respectively,

$$z_0 = \sum_{i=1}^{n} x_i ; \; x_i = 0 \text{ with probability } q \qquad (20)$$
$$x_i = 1 \text{ with probability } (1-q)$$

Also
$$z_i (i \neq 0) = \sum_{i=1}^{n} y_i ; \; y_i = 0 \text{ with probability } (1-p) \qquad (21)$$
$$y_i = 1 \text{ with probability } p$$

The probability p can be identified as (fig. 5) the probability of deciding for a 1 in the case of envelope detection in the presence of noise alone. q is the probability of deciding for a 0 when signal and noise are present. Taking a threshold level b and signal amplitude A, noise variance σ^2

$$q = \int_0^b \gamma \exp\left(-\frac{1}{2}\left(S^2 + \left(\frac{\gamma}{\sigma}\right)^2\right)\right) I_0\left(\frac{\gamma}{\sigma} S\right) d\gamma \qquad (22a)$$

where $S \triangleq A/\sigma$ (signal to noise)

$$= \int_0^{b/\sigma} \xi \exp\left(-\frac{1}{2}\left(S^2 + \xi^2\right)\right) I_0(S\xi)\, d\xi \qquad (22b)$$

This can be identified as the complementary Marcum Q- function[5],

$$q = 1 - Q_1(S, \frac{b}{\sigma}) = 1 - Q_1(S,TS) \tag{23}$$

where $Q_1(\alpha,\beta)$ =>Marcum Q function; $T \triangleq \frac{b}{A}$ (normalized threshold)

p is the simple integral of a Rayleigh density:

$$p = e^{-b^2/2N} = e^{-S^2T^2/2} \tag{24}$$

Now, since z_0 is the sum of n independent x_i's, it is a number between 0 and n and is binomially distributed

$$\text{prob } (z_0 = \alpha) = b(\alpha,n, 1-q) \tag{25a}$$

$$\text{where } b(\alpha,n, 1-q) \triangleq {}^nC_\alpha \, (1-q)^\alpha \, q^{n-\alpha} \tag{25b}$$

is the binomial probability function.

Similarly z_i $(i\neq 0)$ are numbers between 0 and n and are binomially distributed.

$$\text{prob } (z_{\substack{i \\ i\neq 0}} = \beta) = b(\beta, n, p) \equiv {}^nC_\beta (p)^\beta \, (1-p)^{n-\beta} \tag{26}$$

Hence $P_{m,n} = \text{prob } [z_0 < \max (z_1, z_2 \ldots z_m)]$

$$= \sum_\alpha \text{prob}(z_0 = \alpha) \text{ prob } [\text{at least one of } z_i \geq \alpha]_{i\neq 0} \tag{27a}$$

$$= \sum_\alpha \text{prob}(z_0 = \alpha) \, [1-\text{prob}(\text{all of } z_i < \alpha)]_{i\neq 0} \tag{27b}$$

Since the z_i are statistically independent.

$$P_{m,n} = \sum_{\alpha=0}^{n} b \, (\alpha,n, 1-q)\{1-[B(\alpha-1, n, p)]^m\} \tag{22}$$

where B is the cumulative binomial distribution, defined by

$$B(s,n,p) = \sum_{k=0}^{s} b(k,n,p)$$

CALCULATION PROCEDURE:

First p and q are computed for a given signal to noise ratio and threshold. Calculation of q involves Marcum's Q function which is easily bounded using (18) and (19). $P_{m,n}$ can then be computed using the binomial probability and distribution functions. These $P_{m,n}$ terms are summed as in (3). Here again $LP_{1,K}$ was found to be dominant and only a few terms in the sum are actually required even for large L. Results for L=200 and optimum threshold are shown in Fig. 8c. The curves for optimum threshold were obtained by using a minimization routine on P_E for T in the interval (0.0, 1.0). The threshold independence allows easy comparison with other schemes.

3. 'GREATEST-OF' (ORTHOGONAL)

In this detection scheme, shown in Fig. 6, the receiver selects the largest of the envelope detector outputs and assigns it a 1, the rest being taken as zero. The correct and incorrect branch metrics cannot simultaneously be 1, as in the case of hard quantizing. Intuitively, one would expect that for very short constraint lengths (weak coding), this scheme would be superior to hard quantizing since the former is closer to the optimum scheme for the uncoded receiver in the same situation. On the other hand, for longer constraint lengths, the 'greatest-of' receiver discards more information pertinent to the decision and behaves less like the optimum continuous receiver than does the hard quantized receiver. The latter should therefore be superior for large K.

The error probability, ε, on a single tentative decision is the probability of assigning a 1 to an incorrect branch metric. This can be identified as the symbol error probability of an MFSK system, with m frequencies. Thus [6] :

$$\varepsilon = \int_0^\infty x \exp\left[-x^2 + A_c^2/\sigma^2)/2\right] I_0(xA_c/\sigma) \cdot \left[1-\left(1-\exp(-x^2/2)\right)^{m-1}\right]dx \tag{29}$$

ε can be computed from the above or read from available curves.

Since ε is the probability of assigning a 1 to a wrong branch metric $(1-\varepsilon)$ is the probability that the correct branch's metric is 1. Hence

$$\text{prob}\ (z_0 = \alpha) = b(\alpha, n, 1-\varepsilon) \tag{30}$$

and since all the signals are selected in a mutually exclusive way, the probability of any given one of the 2^K-1 wrong signals being selected is

$$p = \frac{\epsilon}{2^K-1} \tag{31}$$

Hence

$$\text{prob}\ (z_i = \beta) = b\left(\beta, n, \frac{\varepsilon}{2^K-1}\right) \tag{32}$$
$$i\neq 0$$

The rest is similar to the hard quantizing case previously described, and the calculation can be completed using (30) and (32) along with (22) and (3), to find $P_{m,n}$ and P_E.

CALCULATION PROCEDURE:

Since ε is fairly difficult to compute directly, P_E was found as a function of ε, using the binomial probability and distribution functions. Then, curves for signal to noise ratio vs. ε[6], were used to plot P_E as a function of signal to noise ratio. Results are shown in Fig. 8d.

QUASI-ORTHOGONAL TREE CODES:

A logical extension to orthogonal tree codes that would permit smaller bandwidth expansion is a tree code that uses quasi-orthogonal signals. In particular, the signal set $\{S_0, S_1 \ldots S_{2^K-1}\}$ would consist of PN sequences, Gold codes, etc.. The choice would depend on the allowable correlation properties of the signal set.

As for the orthogonal case, we shall investigate the performance of both incoherent detection and coherent detection.

B. INCOHERENT QUASI-ORTHOGONAL SCHEMES:

1. Continuous (Quasi-orthogonal):

The receiver structure is the same as that shown in Fig. 3. For the continuous case the branch metrics can take on a continuum of values.

We now assume that A_c is the auto-correlation of any signals $S_i(t)$, and that K_c is the cross-correlation (or its upper bound) of any pair of signals $\{S_i(t), S_j(t); j \neq i\}$. If the upper bound is used, we obtain an overestimate of the error probability.

From the receiver structure it can be seen that the reduced metric of a correct path is

$$z_0 = \sum_{i=1}^{n} (A_c \cos\theta_i + x_i)^2 + \sum_{i=1}^{n} (A_c \sin\theta_i + y_i)^2 \qquad (33)$$

where x_i, y_i are zero mean Gaussian random variables with variance σ^2.

The reduced metric $z_i (i \neq 0)$ for an incorrect path is

$$z_{\substack{i \\ i \neq 0}} = \sum_{j=1}^{n} (K_c \cos\theta_j + x_j)^2 + \sum_{j=1}^{n} (K_c \sin\theta_j + y_j)^2 \qquad (34)$$

where x_j, y_j are zero mean G.R.V.s with variance σ^2.

This can be used to find $P_{m,n}$ using (9), where:

$f_{z_0}(\alpha)$ is the non central χ^2 density with noncentral parameter nA_c^2 and 2n degrees of freedom

$f_{z_i}(\alpha)$ $(i\neq 0)$ the noncentral χ^2 density with noncentral parameter nK_c^2 and 2n degrees of freedom.

It can be noted here that this differs from the orthogonal case in that z_i $(i\neq 0)$ is now noncentral χ^2 instead of just χ^2 distributed. One would expect this to result in some degradation in performance, depending on the value of K_c.

Substituting the above $f_{z_0}(.)$ and $f_{z_1}(.)$ in (9), we obtain:

$$P_{m,n} = \int_0^\infty dq_2\, f_{z_{max}}(q_2)\, \{1-Q_n(\tfrac{\sqrt{n}A_c}{\sigma}, \tfrac{\sqrt{q_2}}{\sigma})\} \tag{35a}$$

$$= m \int_0^\infty dq_2\, f_{z_1}(q_2) \cdot [F_{z_1}(q_2)]^{m-1} \{1-Q_n(\tfrac{\sqrt{n}A_c}{\sigma}, \tfrac{\sqrt{q_2}}{\sigma})\} \tag{35b}$$

$F_{z_1}(q_2)$ can be expressed in terms of the complementary Q function mentioned earlier, which reduces the above to:

$$P_{m,n} = m \int_0^\infty dq_2\, f_{z_1}(q_2)\, [1-Q_n(\tfrac{\sqrt{n}K_c}{\sigma}, \tfrac{\sqrt{q_2}}{\sigma})]^{m-1} \cdot [1-Q_n(\tfrac{\sqrt{n}A_c}{\sigma}, \tfrac{\sqrt{q_2}}{\sigma})] \tag{35c}$$

Substituting

$$f_{z_1}(\alpha) = \frac{1}{2\sigma^2} \left(\frac{\alpha}{nK_c^2}\right)^{\frac{n-1}{2}} \exp\left(-\frac{nK_c^2+\alpha}{2\sigma^2}\right) I_{n-1}\left\{\frac{(\alpha nK_c^2)^{1/2}}{\sigma^2}\right\} \tag{36}$$

and letting $\eta = \frac{\sqrt{n}K_c}{\sigma}$, $x = \frac{\alpha}{2\sigma^2}$, $S \triangleq \frac{A_c}{\sigma}$, $S' \triangleq \frac{K_c}{\sigma}$

$$P_{m,n} = \int_0^\infty dx\ p(x)\ \exp(-x)$$

where $$p(x) = \left(\frac{2x}{\eta^2}\right)^{\frac{n-1}{2}} \exp\left(-\frac{\eta^2}{2}\right) I_{n-1}(\eta\sqrt{2x}) \cdot \{1-Q_n(\eta,\sqrt{2x})\}^{m-1} \{1-Q_n(\sqrt{n}S, \sqrt{2x})\} \cdot m \qquad (37)$$

$$\eta \triangleq \frac{\sqrt{n}K_c}{\sigma} = \frac{\sqrt{n}A_c}{\sigma} \cdot \frac{K_c}{A_c} = \frac{\sqrt{n}S}{\mu} = \sqrt{n}S'$$

where $\mu \triangleq \frac{A_c}{K_c}$ auto correlation to cross correlation ratio

It can be expected that as μ becomes larger, the quasi orthogonal tree code reduces to an orthogonal one, and that error probability obtained from the above for large μ should be nearly equal, but a little greater than that obtained from (17).

CALCULATION PROCEDURE:

The integral (37) was evaluated numerically using a 10 point Gauss-Laguerre quadrature integration formula. The Q function was computed using the bound mentioned earlier. Results for this case are shown in Fig. 8f.

2. HARD QUANTIZING (QUASI-ORTHOGONAL)

The error probability is easily evaluated in this case using the Binomial distribution. With reference to the analysis for hard quantizing discussed earlier, it can be seen that p and q (p is the probability of assigning a 1 to an incorrect branch metric and q is the probability of assigning a 0 to the correct branch metric) are both obtained from Rician

densities. Referring to Fig. 7, we observe that

$$q = 1 - Q_1 (S, TS) \tag{38}$$

as before

and

$$p = \int_b^\infty \gamma \exp\left(-\frac{1}{2}\left(S' + \left(\frac{\gamma}{\sigma}\right)^2\right)\right) I_0\left(\frac{\gamma}{\sigma} S'\right) d\gamma \tag{39a}$$

where $S' \triangleq \frac{K_c}{\sigma}$

$$= Q_1(S', b/\sigma) \tag{39b}$$

$$\text{If } \mu \triangleq \frac{A_c}{K_c}, \quad p = Q_1\left(\frac{S}{\mu}, TS\right) \tag{40}$$

Once p and q are obtained from the above, the rest of the analysis and calculation procedure is analogous to the hard quantizing case discussed earlier, and the calculation can be completed using (28) and (3).

COHERENT SCHEMES:

In order to compare the incoherent schemes with coherent ones, these were also analyzed in a manner similar to the above.

C. COHERENT ORTHOGONAL SCHEMES:

1. CONTINUOUS ORTHOGONAL

Even though an exponential bound has been obtained for this case in [3], we compute P_E by summing $P_{m,n}$ terms so that a more direct comparison to the other schemes considered is obtained.

$$P_{m,n} = \int_{-\infty}^{\infty} dq_2 \int_{-\infty}^{q_2} dq_1 \; f_{z_0}(q_1) \; f_{z_{max}}(q_2)$$

where Z_0 is unit variance Gaussian with mean $\sqrt{n}S$ and $z_{max} \triangleq \max(z_1, z_2 \ldots z_m)$, $z_i (i \neq 0)$ being independent Gaussian random variables with zero mean and unit variance.

This reduces to

$$P_{m,n} = \frac{m}{\sqrt{\pi}} \int_{-\infty}^{\infty} \exp(-\xi^2) H^{m-1}(\sqrt{2}\xi) G(\sqrt{2}\xi) d\xi \qquad (41a)$$

where G(x) is the unit variance Gaussian cumulative distribution function with mean $\sqrt{n}S$ and H(x) is the unit variance Gaussian c.d.f. with mean 0. In terms of error functions:

$$\begin{aligned} H(x) &= .5 + \text{erf}\left(\frac{x}{\sqrt{2}}\right)/2 && \text{if } x > 0 \\ &= .5 && \text{if } x = 0 \\ &= .5 - \text{erf}\left(-\frac{x}{\sqrt{2}}\right)/2 && \text{if } x < 0 \end{aligned}$$

$$\begin{aligned} G(x) &= .5 + \text{erf}\left(\frac{x-a}{\sqrt{2}}\right)/2 && \text{if } x > a \\ &= .5 && \text{if } x = a \\ &= .5 - \text{erf}\left(\frac{a-x}{\sqrt{2}}\right)/2 && \text{if } x < a \end{aligned} \qquad (41b)$$

$$\text{where erf}(\xi) \triangleq \frac{2}{\sqrt{\pi}} \int_0^{\xi} e^{-y^2} dy$$

The above integral was numerically evaluated using a 10 point Gaussian Hermite formula. Results are shown in Fig. 8a.

2. HARD QUANTIZING (ORTHOGONAL):

In this case, p and q (where they have the same meaning as before) are found from.

$$p = 1 - H(TS)$$
$$q = G(TS) \qquad (42)$$

where H and G are defined as in (41b)

The remaining calculation can be completed with (28) and (3). Results are shown in Fig. 8b.

3. GREATEST OF (ORTHOGONAL)

The coherent case is identical to the incoherent one in terms of ε, the error probability of an MFSK system. The only difference now is that the curves of P_E vs. SNR must be obtained using the ε vs. SNR curves for coherent MFSK [6].

D. COHERENT QUASI-ORTHOGONAL :

1. CONTINUOUS (QUASI-ORTHOGONAL):

This case is easily handled in a manner similar to coherent continuous (orthogonal) by recognizing that $P_{m,n} = \text{prob}\,[z_0 < \max(z_1, z_2 \ldots z_m)]$ where z_0 and z_i $(i \neq 0)$ are unit variance Gaussian random variables with mean $\sqrt{n}S$ and $\sqrt{n}S'$ respectively ($S \triangleq A_c/\sigma$, $S' \triangleq K_c/\sigma$). Results are shown in Fig. 8f.

2. HARD QUANTIZING (QUASI-ORTHOGONAL)

This scheme can be analysed in a manner identical to coherent hard quantizing (orthogonal) by recognizing that the correct and incorrect branch metrics are now centered about A_c and K_c instead of A and 0. Thus p and q can be found from (42) with A replaced by $A_c - K_c$ or S replaced by $S(1-\mu)$. This corresponds to a shift of $20 \log \frac{\mu}{\mu - 1}$ dB on the signal to noise ratio

scale. As expected, for $\mu >> 1$, the performance is identical to the orthogonal one since $\mu/(\mu-1) \rightarrow 1$.

III. COMPARISON OF PERFORMANCE:

The results of the error probability calculation for the various cases described are shown in Fig. 8. In this section we mention a few noteworthy points about the obtained curves.

(1) Fig. 8(a) shows that incoherent detection results in a 2-3 dB degradation, and that the asymptotic performance of the coherent and incoherent systems is equivalent, since the curves are essentially parallel for large SNR.

(2) Error probability P_E decreases as constraint length K is increased From the even separation between the curves for K=3,4,5,6,7 it may be inferred that P_E decreases in an exponential way. The decrease in P_E is greater for increased SNR, a property which has been pointed out in [2].

(3) From Fig. 8(b) it can be seen that P_E increases with block length L. In the expression for P_E (3), the term $LP_{1,K}$ predominates, and a linear increase in P_E can be expected. This is borne out by the even separation of the curves for exponentially increasing L in Fig. (6). It can be noted that P_E is insensitive to L and having shown this, we consider curves only for L=200.

(4) Fig. 8(c) shows that the degradation caused by incoherent detection is 2-3 dB for hard quantizing also. The general nature of the curves is the same as for the continuous case, and the previous observations still apply.

(5) Fig. 8(d) shows P_E curves for 'greatest-of' detection. The improvement

with K is found to decrease with increasing K, since the curves tend to bunch closer.

(6) Fig. 8(e) shows how the three incoherent schemes compare. As expected, the continuous case yields the lowest P_E for a given SNR. The degradation due to hard quantizing is seen to be about 2-3 dB over most of the range. Except for this shift in SNR, the continuous scheme is essentially equivalent to the hard quantizing one; the curves have the same general nature and are parallel. The 'greatest-of' scheme is better than hard quantizing for small K, but the advantage decreases as K increases. K = 3 is about 2 dB better, but K = 7 is typically less than 1 dB better. The choice between these two schemes could then be dictated by the constraint length of the code.

(7) Fig. 8(f) shows the quasi-orthogonal continuous case as compared with the orthogonal one. It is found that even for a low ratio of auto correlation to cross correlation such as 8, the degradation is typically only .2- .4 dB. For large A_c/K_c such as 256, the quasi-orthogonal system should be essentially equivalent to the orthogonal ones; this is borne out by the results which show the curves for A_c/K_c =256 just above the orthogonal curves. These results show that for a slight SNR degradation a significant bandwidth saving is possible by using quasi-orthogonal codes instead of strictly orthogonal ones.

(8) Fig. 8(g) shows the same set of curves as (f) for hard quantized quasi-orthogonal. The degradation is somewhat greater in this case, but this is an overestimate because of an additional bound used (evaluation of p from (40) using (18)) in computing P_E for the hard quasi-orthogonal case.

IV. QUASI-ORTHOGONAL TREE CODES FOR MULTIPLE ACCESS:

We consider briefly an example application of quasi-orthogonal tree codes to multiple access. The possibility of using orthogonal convolutional codes for multiple access has been discussed in [12], in which several low duty cycle users employing on-off signalling are considered. Here we analyze the performance of a multiple access scheme which uses incoherent detection and a quasi-orthogonal tree code. It is assumed that other user interference is the dominant source of noise.

A simple way to achieve multiple access is to allow all users to transmit simultaneously, using the same signal set. The encoder for each user adds a K bit portion of a unique pseudo noise sequence to the contents of the K bit shift register in Fig. 1, and uses the sum to select a signal $S_j(t)$ $(j=0,1..2^K-1)$. [12] This makes other user interference appear like random noise and may be thought to have the effect of providing each user with a different code. The use of orthogonal signals for the tree code is, of course, desirable, but for a code of constraint length K, a bandwidth expansion of 2^K is required. On the other hand, suitable choice of a family of mutually quasi-orthogonal signals (such as Gold codes) can provide 2^K signals with a bandwidth expansion substantially less than 2^K, though with some degradation in performance. This motivates the use of a quasi-orthogonal tree code for multiple access.

The receiver for any user is identical to that in Fig. 3; however, the branch metric corresponding to channel i is now interpreted as the branch metric for channel $(i- \langle pn \rangle) \bmod 2^K$ where $\langle pn \rangle$ is the value of the K bit portion of the sequence added at the encoder. Thus the receiver must have a synchronous copy of the PN sequence being generated at the encoder. The expanded version of one channel of the receiver is shown in Fig. 9. We assume that M users are transmitting simultaneously and that in a signalling interval user j sends $S_{i_j}(t)\cos(\omega_0 t+\theta_j)$. $S_{i_j}(t)$ is the signal on the code tree sent out by user j, and is assumed to be any of the signals $\{S_i,\ i=0,1...2^K-1\}$ with equal probability. θ_j is a random phase associated with

user j's carrier, and is assumed to be uniformly distributed. The composite received signal $(r(t)$ at any receiver is given by

$$r(t) = S_{i_1}(t)\cos(\omega_0 t + \theta_1) + S_{i_2}(t)\cos(\omega_0 t + \theta_2) + \cdots + S_{i_M}(t)\cos(\omega_0 t + \theta_M) \tag{43}$$

Consider now receiver 1 where $S_{i_1} = S_0$. The output of the matched filter on the channel corresponding to S_0 is $v^0(t)$, where the superscript refers to channel 0. This can be expressed as a desired signal part and a "noise" part due to other user interference. The matched filter output peaks at $t=t_0$.

$$v_0^0(t) = A_c\cos(\omega_0 t_0 + \theta_1) + \sum_{i=2}^{M} x_i\cos(\omega_0 t_0 + \theta_i) \tag{44}$$

where $x_i = A_c$ with probability $1/2^K$

$= K_c$ with probability $1-1/2^K$

This is because the peak output of the matched filter due to the interfering signals S_{i_j} $(j\neq 1)$ is the cross correlation of S_0 and S_{i_j}. Now $< S_0(t) \cdot S_{i_j}(t) > = A_c$ if $S_{i_j} = S_0$ and is equal to K_c if $S_{i_j} \neq S_0$. Using the assumption that S_{i_j} is any of 2^K signals on the tree with equal probability we obtain (44)

Hence the two components y_c and y_s on channel 0 can be expressed as

$$y_c^0 = A_c\cos\theta_1 + \sum_{i=2}^{M} x_i\cos\theta_i \triangleq A_c\cos\theta_1 + n_c$$
$$y_s^0 = A_c\sin\theta_1 + \sum_{i=2}^{M} x_i\sin\theta_i \triangleq A_c\sin\theta_1 + n_s \tag{45}$$

The quantities n_c and n_s are random terms representing the noise due to other user interference. The variance of this noise is

$$\sigma_n^2 = \sigma_{n_s}^2 = \sigma_{n_c}^2 = E\left(\sum_{i=2}^{M} x_i \cos\theta_i\right)^2 \tag{46a}$$

$$= \frac{M-1}{2^{K+1}}\{A_c^2 + (2^K-1)\,K_c^2\} \tag{46b}$$

using the fact that x_i and θ_i are independent and that θ_i is uniformly distributed.

Similarly, the matched filter output on an incorrect channel, say channel 1, is $v^1(t)$ and is given by,

$$v^1(t_0) = K_c\cos(\omega_0 t + \theta_1) + \sum_{i=2}^{M} x_i \cos(\omega_0 t_0 + \theta_i) \tag{47}$$

The y_c and y_s components are therefore:

$$\begin{aligned} y_c^1 &= K_c\cos\theta_1 + \sum_{i=2}^{M} x_i\cos\theta_i \triangleq K_c\cos\theta_1 + n_c \\ y_s^1 &= K_c\sin\theta_1 + \sum_{i=2}^{M} x_i\sin\theta_i \triangleq K_c\sin\theta_1 + n_s \end{aligned} \tag{48}$$

If now, we assume that the random variables n_c and n_s are Gaussian, which is reasonable if M, the number of users, is large, the above can be used to compute P_E for a given number of users, M by using (37) where,

$$S \triangleq \frac{A_c}{\sigma_n} = \left[\frac{2^{K+1}}{(1+(2^K-1)/\mu^2)(M-1)}\right]^{1/2} \tag{49}$$

and

$$S' \triangleq \frac{K_c}{\sigma_n} = \frac{S}{\mu}$$

($\mu \triangleq \frac{A_c}{K_c}$: ratio of auto correlation to cross correlation).

PERFORMANCE USING GOLD CODES:

We now obtain performance curves for the multiple access scheme analyzed above for a specific family of quasi-orthogonal signals. Since Gold codes are widely used for multiple access schemes and have the property of providing large families of sequences with relatively low mutual cross-correlation, we use these for this example. A measure of the multiple access capability of a system is the bandwidth expansion per user ($\mathcal{E}$), needed to maintain a given error probability, P_E. Such curves of P_E vs. $\mathcal{E}$ are obtained in a manner described below.

In [14] it is shown that 2^n+1 distinct Gold sequences, each of length 2^n-1 can be generated with a 2 register Gold code generator of length n. Also, the cross-correlation function K_c is upper bounded by

$$|K_c| < \left\{ \begin{array}{ll} 2^{(n+1)/2} + 1 & \text{for n odd} \\ 2^{(n+2)/2} + 1 & \text{for n even} \end{array} \right\} \qquad n \neq \text{mod4} \tag{50}$$

Hence the ratio of auto correlation to cross-correlation (μ) can be lower bounded for a given n, since auto-correlation $A_c = 2^n-1$ (length of the sequence).

To construct a tree of constraint length K using the above Gold code families, 2^K signals are needed. If timing information is available at the receivers, a total of $(2^n+1)\ (2^n-1)$ usable signals result, since there are 2^n-1 cyclic shifts of each of 2^n+1 sequences. Hence n must satisfy the inequality,

$$(2^n+1)\ (2^n-1) = 2^{2n}-1 \geq 2^K \tag{51}$$

which yields $n > K/2$; n is at least the smallest integer greater than K/2. The corresponding bandwidth expansion is equal to the length of the sequences and is 2^n-1. We obtain curves of P_E vs. $\mathcal{E}$ ($\mathcal{E}=(2^n-1)/M$) using the above and (49) for given K and various $n > K/2$. It may be observed that for n odd, the cross-correlation bound is lower in (50). Performance is found to improve as the constraint length, K, increases, keeping n as close to K/2 as possible seems advantageous, since for a given K, lower n gives better performance. Typically a K=10, n=7 system can support about 10 users at an error probability of 10^{-5}. Note that this is the block error probability for L = 200, and is always much greater than bit error probability.

V. CONCLUSION:

Performance curves for orthogonal tree codes using various detection schemes, both coherent and incoherent, have been obtained. In addition, the effect of using a quasi-orthogonal signal set in place of an orthogonal one has been considered. The results indicate that a substantial saving in bandwidth in exchange for a moderate increase in power becomes possible An example application of quasi-orthogonal tree codes to multiple access has been presented. Other schemes for multiple access using quasi-orthogonal tree codes are being investigated and will be considered in a separate paper.

REFERENCES:

1) A.J. Viterbi; "Convolutional codes and their performance in communication systems", IEEE Trans. on Comm. Tech. Oct.1971, pp 751-772.

2) J.A. Heller and I.M. Jacobs, "Viterbi decoding for satellite and space communication", IEEE Trans. on Comm. Tech, Oct.1971, pp 835-848.

3) A.J. Viterbi, "Orthogonal tree codes for communication in the presence of white gaussian noise", IEEE Trans. on Comm. Tech., April1967 pp 238-242.

4) Whalen, "Detection of Signals in Noise", Academic Press 1971, pp 109-118.

5) S.S. Rappaport, "Computing approximation for the generalized Q-function and its complement", IEEE Trans. on Info. Theory, July1971, pp 497-498.

6) Panter, "Modulation, Noise and Spectral Analysis", McGraw Hill 1965 pp 715-717.

7) H.E. Salzer and R. Zucker, "Table of zeros and weight factors of the first fifteen Laguerre polynomials", Bul. Amer. Math. Soc., vol. 55, 1949) pp 1004-1012.

8) H.E. Salzer, R. Zucker and R. Capuano, "Table of the zeros and weight factors of the first twenty Hermite polynomials", J. Res. Nat. Bur. Standards, vol. 48 (1952), pp 111-116.

9) V.I. Krylov, "Approximate Calculation of Integrals", Macmillan, 1962, pp, 129-132 and 343-352.

10) G.H. Robertson, "Computation of the non-central Chi squared distribution", BSTJ vol. 48, Jan.1969, pp 201-209.

11) Brennan & Reed. "Recursive method of computing the Q function", IEEE Trans. on Info. Theory, Apr.1965, pp 312-313.

12) A.R. Cohen, J.A. Heller and A.J. Viterbi, "A new coding technique for multiple access communication", IEEE Trans. on Comm. Tech., Oct.1971 pp 849-855.

13) Dixon, "Spread Spectrum Systems", Wiley Interscience 1976.

14) R. Gold, "Optimal binary sequences for spread spectrum multiplexing", IEEE Trans. on Info. Theory, Oct. 1967, pp. 619-621.

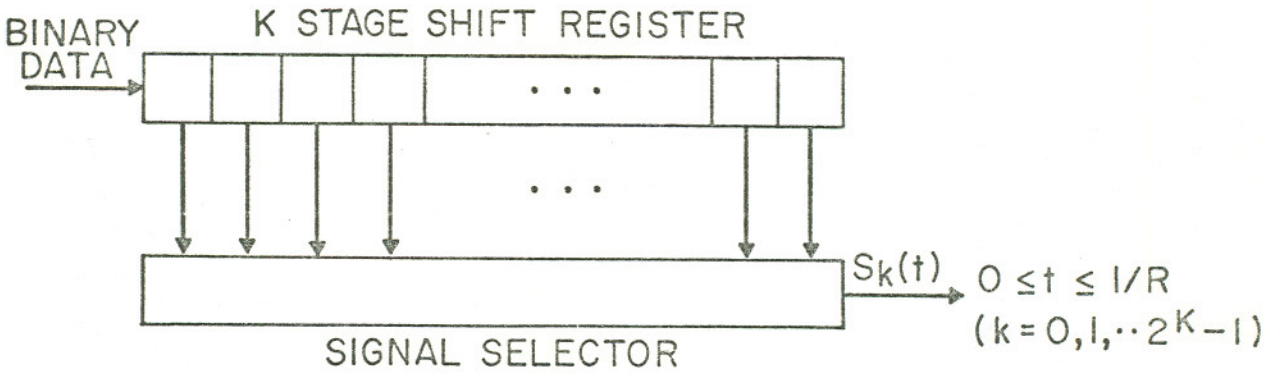

Fig. 1. CONVOLUTIONAL ENCODER FOR TREE CODES.

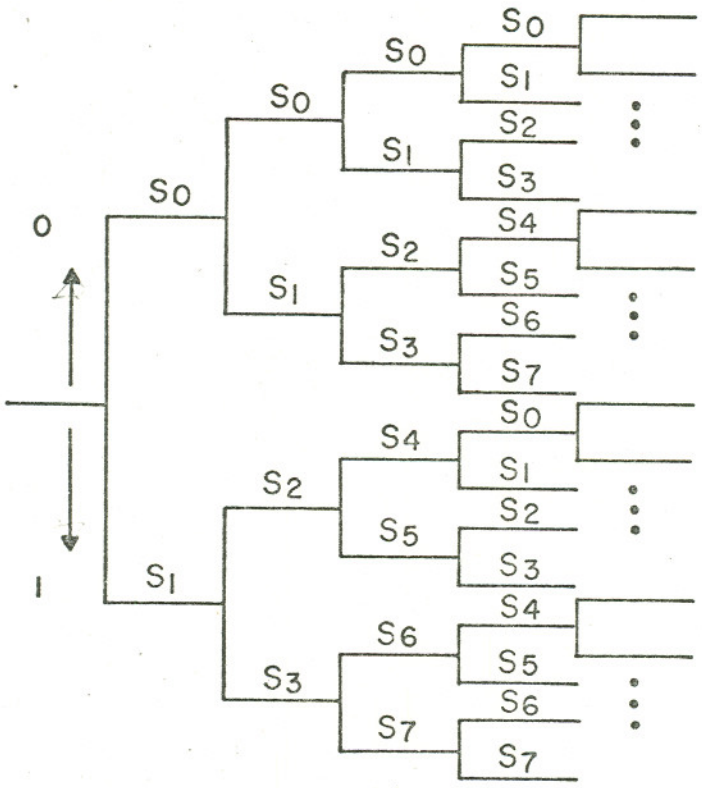

Fig. 2. CODE TREE FOR K = 3

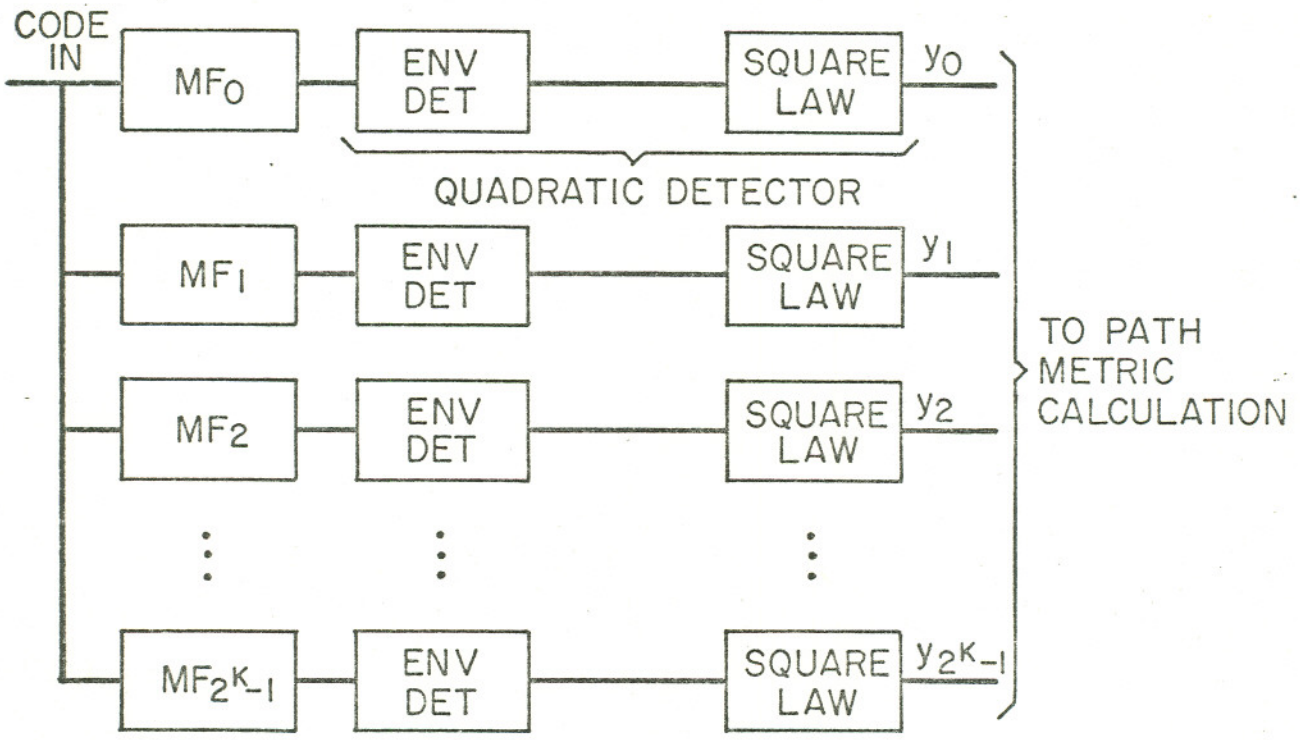

Fig. 3. RECEIVER STRUCTURE FOR INCOHERENT CONTINUOUS CASE

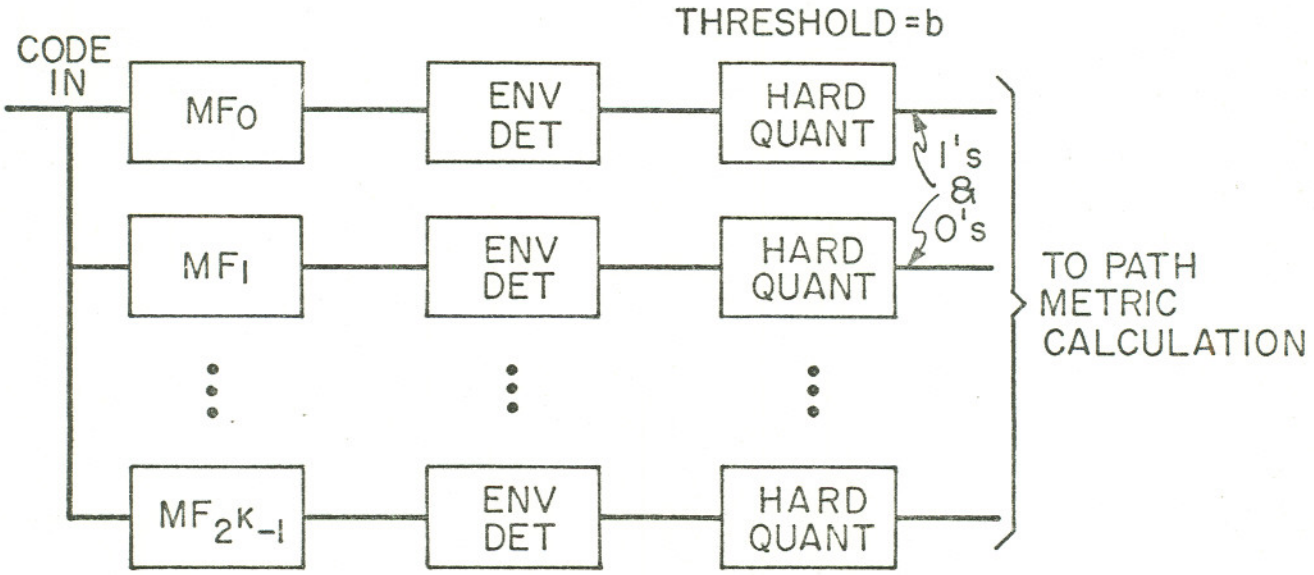

Fig. 4. RECEIVER STRUCTURE FOR INCOHERENT HARD QUANTIZING CASE

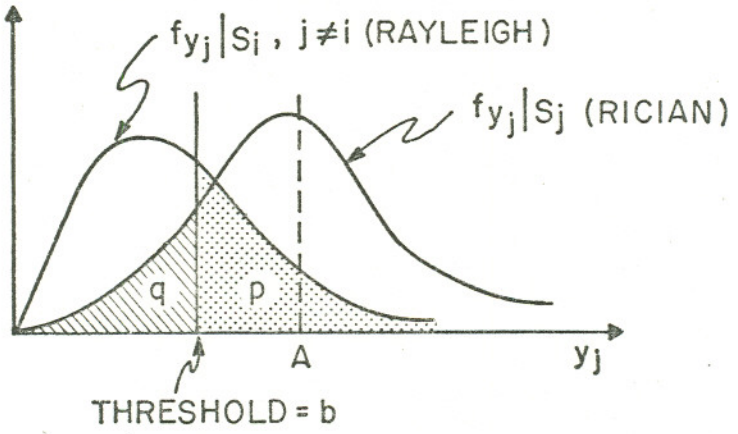

Fig. 5. "p" & "q" FOR ORTHOGONAL HARD QUANTIZING

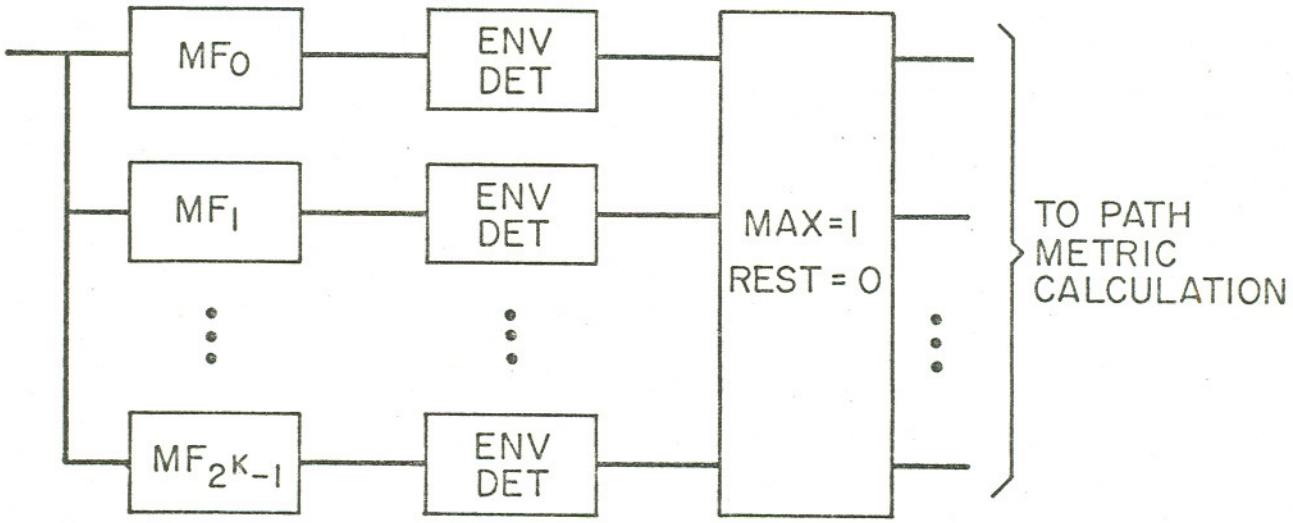

Fig. 6. RECEIVER STRUCTURE FOR INCOHERENT "GREATEST OF" CASE

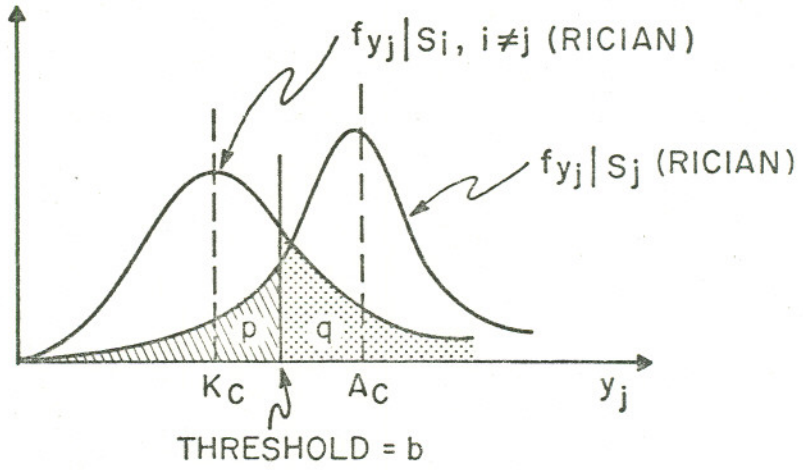

Fig. 7. "p" & "q" FOR QUASI-ORTHOGONAL HARD QUANTIZING

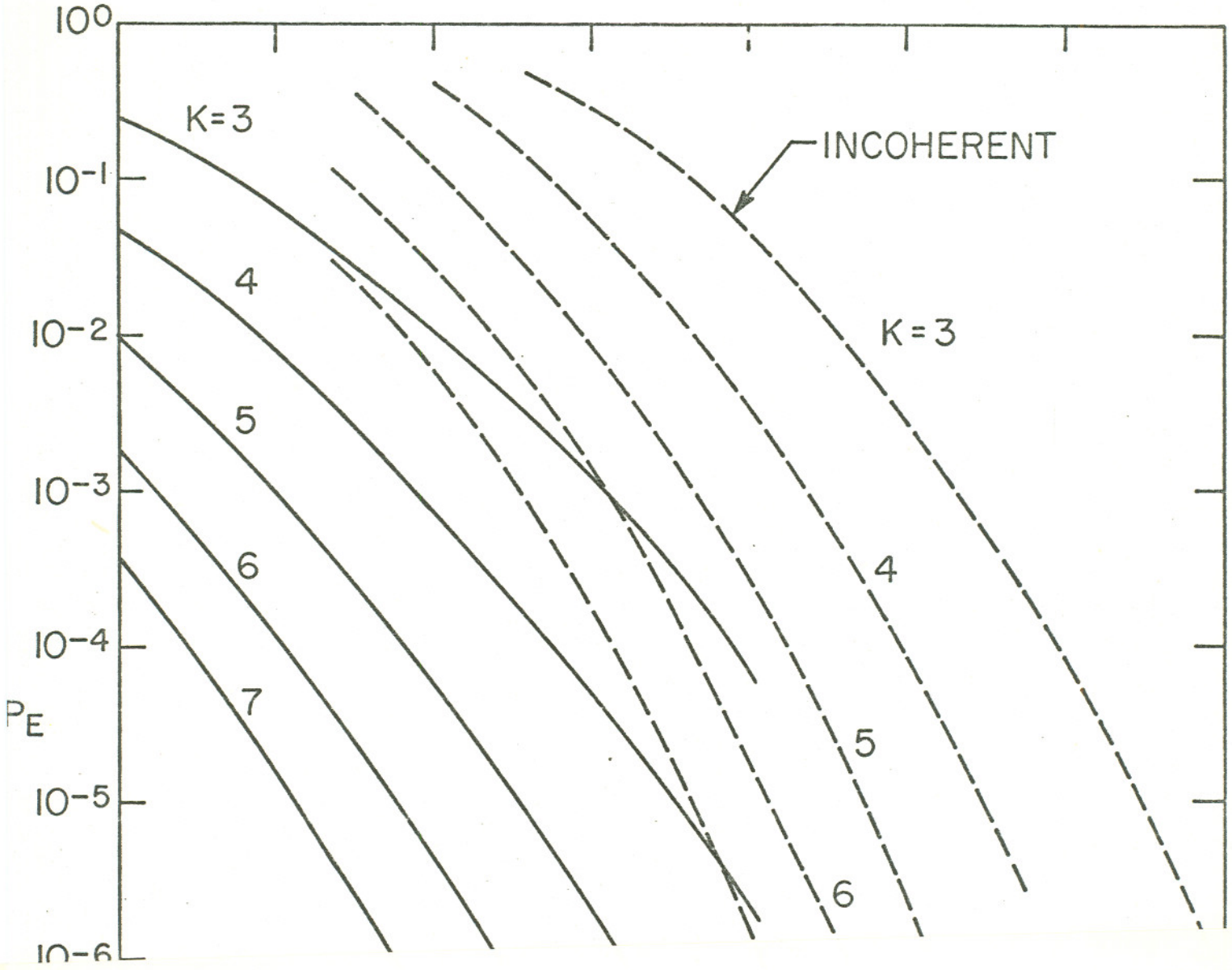
100
10-1
10-2
10-3
10-4
10-5
10-6
PE
K=3
4
5
6
7
INCOHERENT
K=3
4
5
6

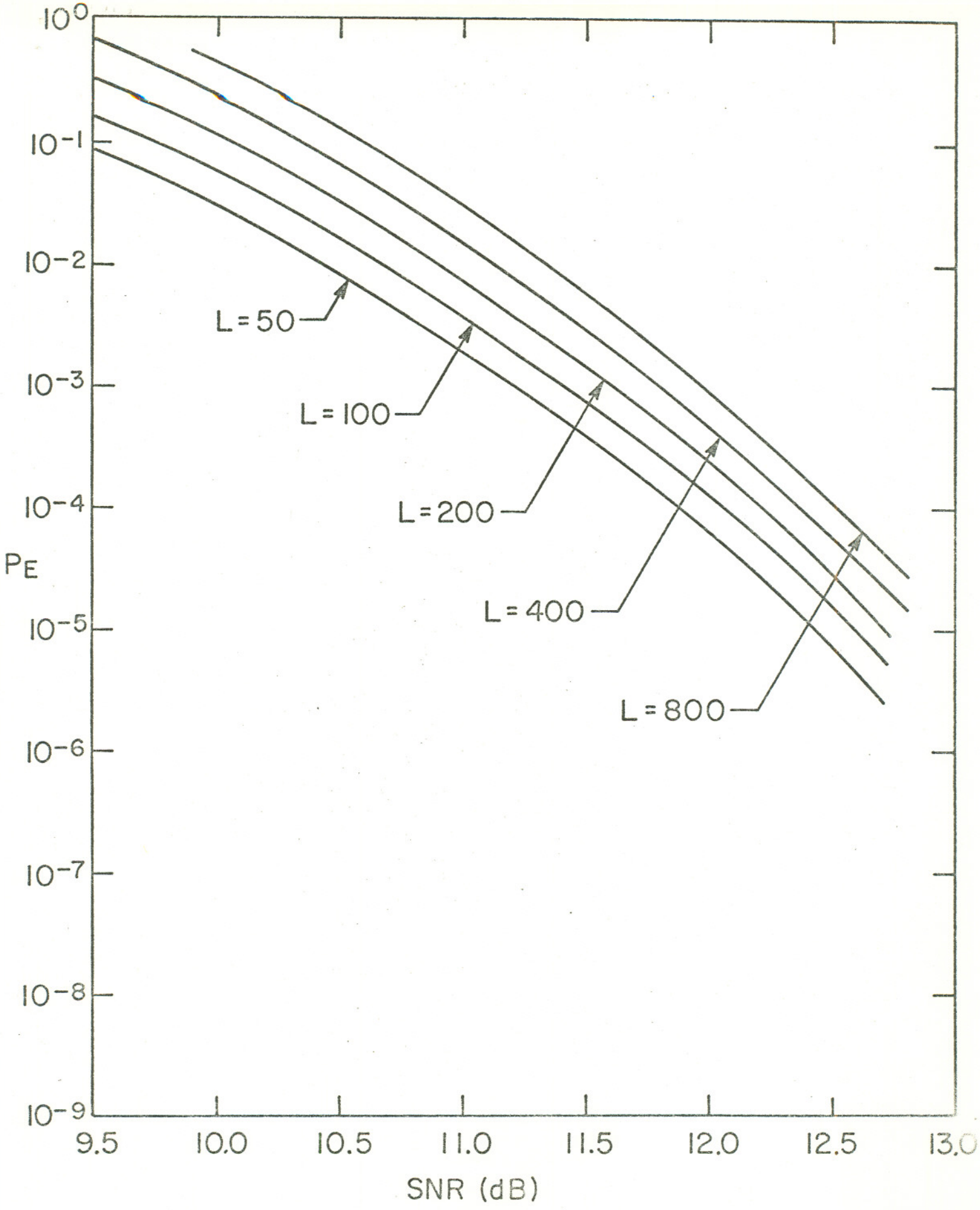

Fig. 8b. ERROR PROBABILITY FOR CONTINUOUS INCOHERENT ORTHOGONAL SCHEMES (K = 5, VARIOUS L)

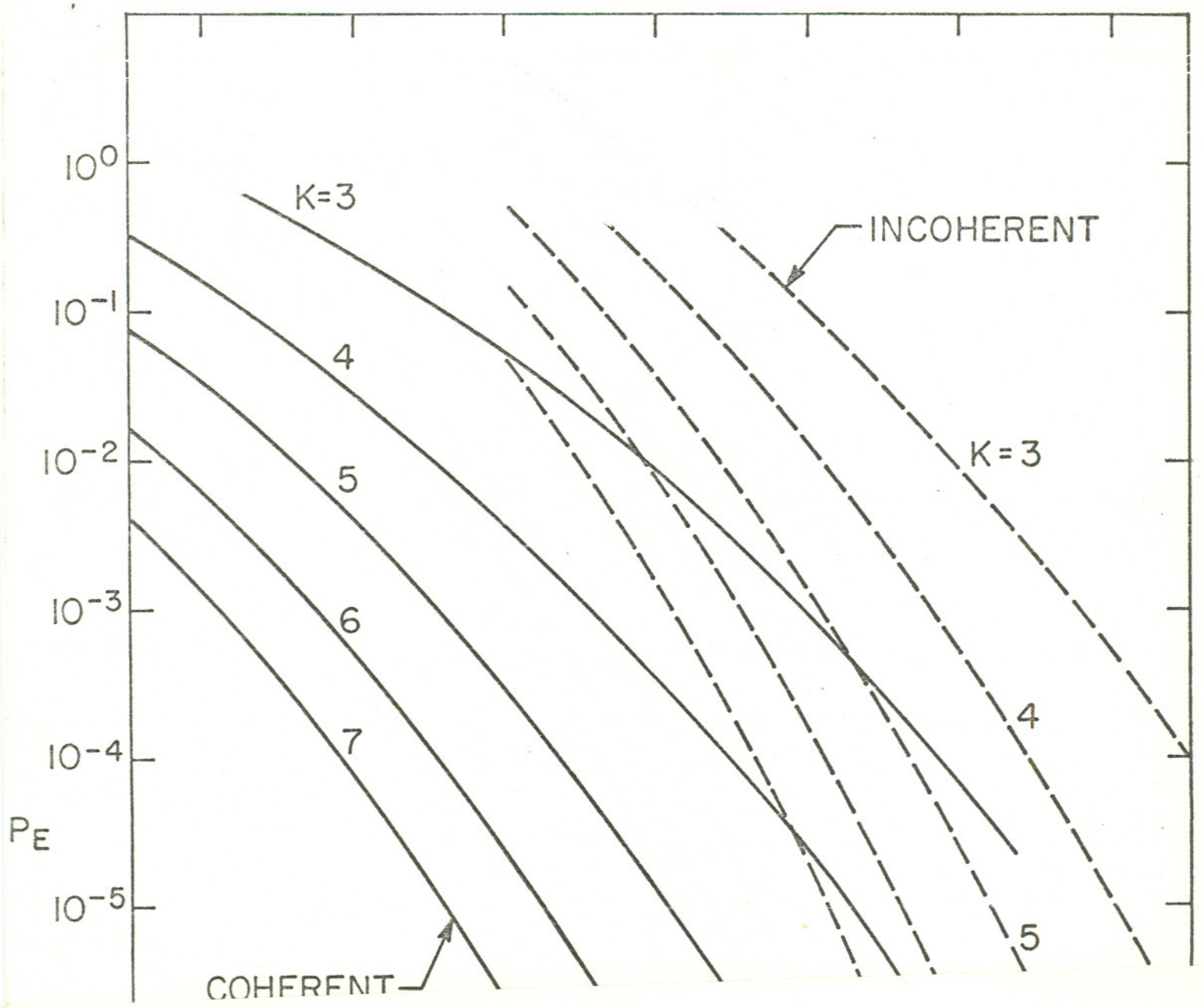
10^0
10^{-1}
10^{-2}
10^{-3}
10^{-4}
10^{-5}
P_E
K=3
4
5
6
7
COHERENT
INCOHERENT
K=3
4
5

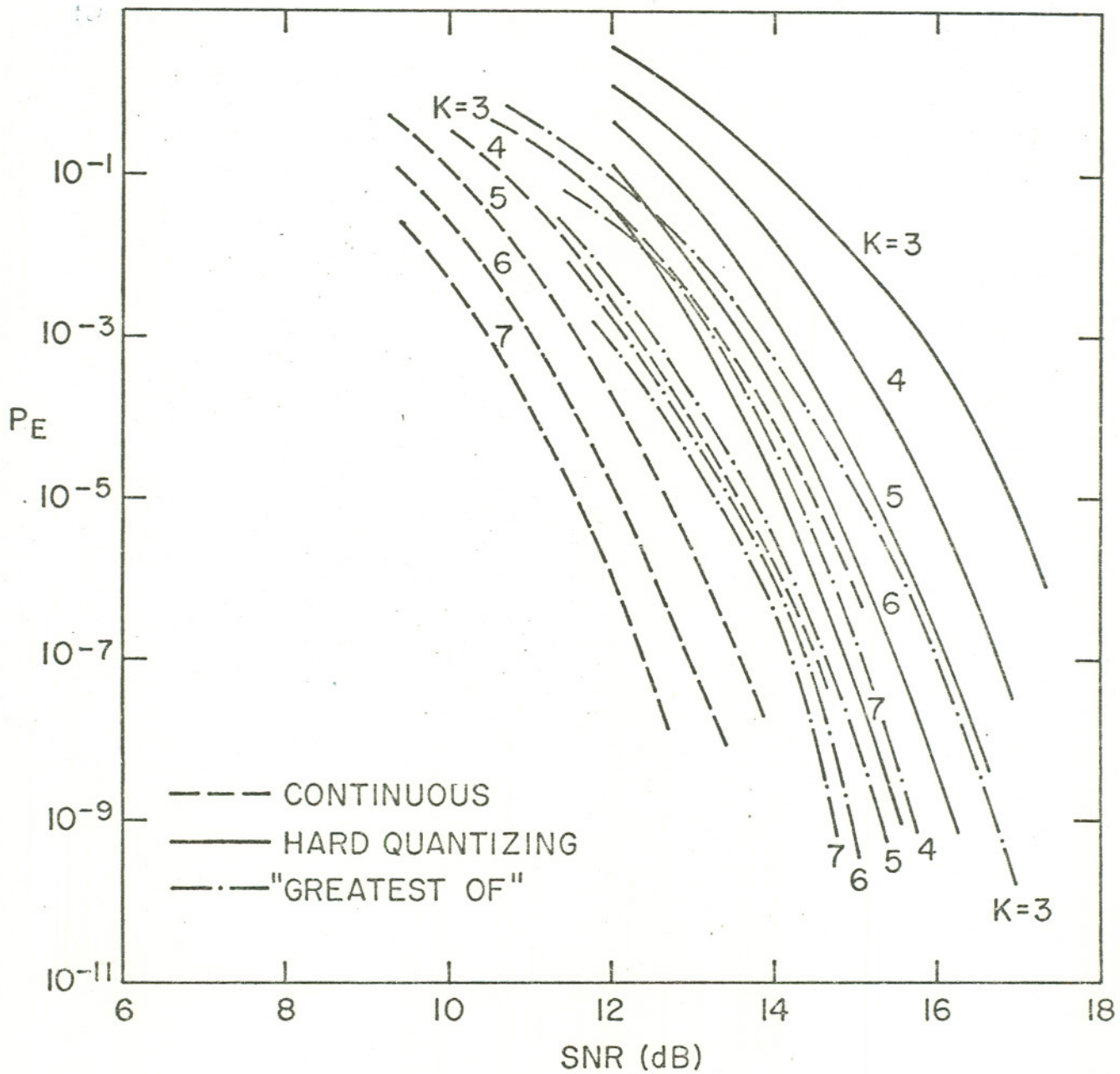

Fig. 8e. COMPARISON OF INCOHERENT ORTHOGONAL SCHEMES (L=200)

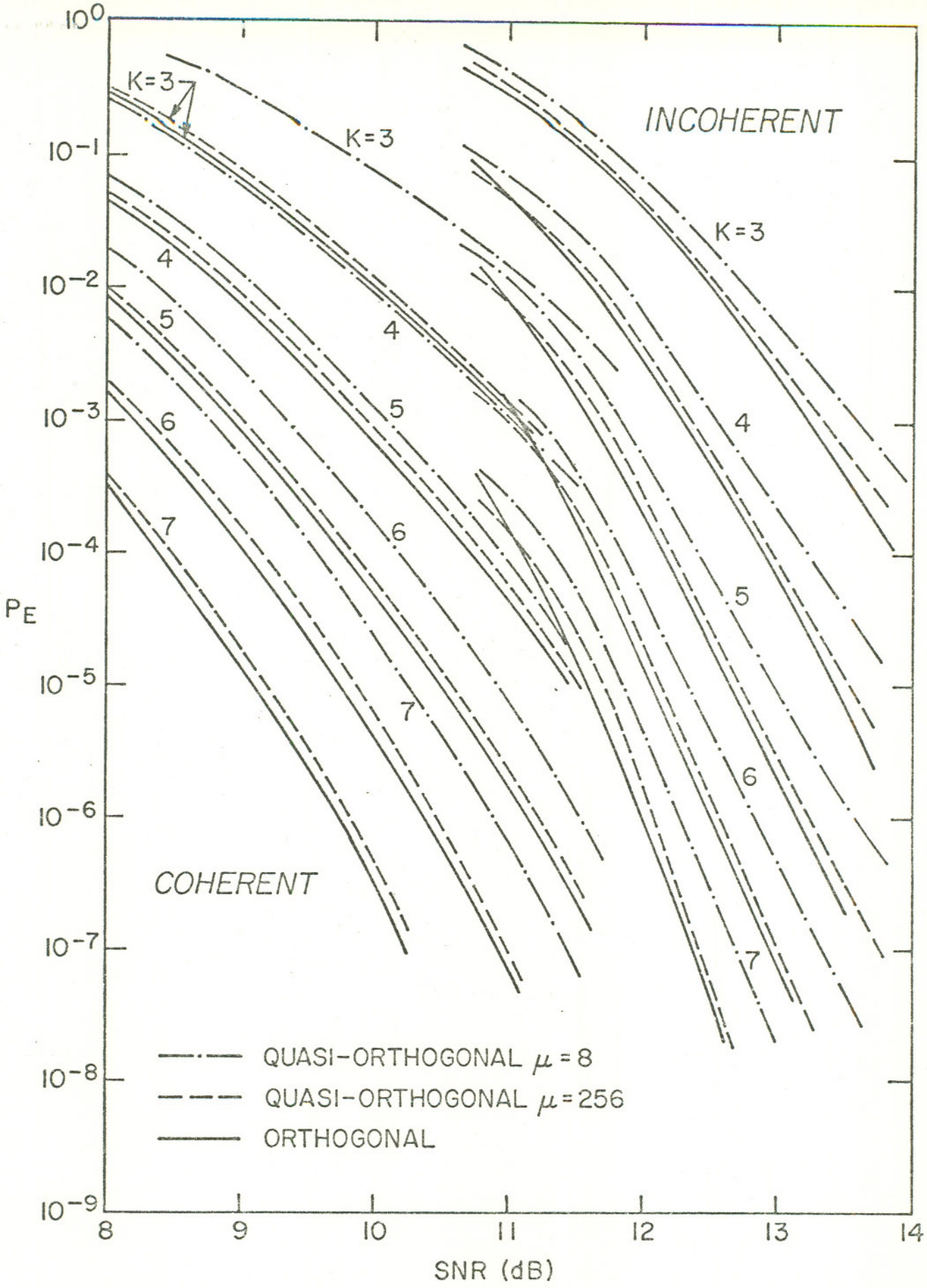

Fig. 8f. COMPARISON OF ORTHOGONAL AND QUASI-ORTHOGONAL CONTINUOUS SCHEMES (L=200)

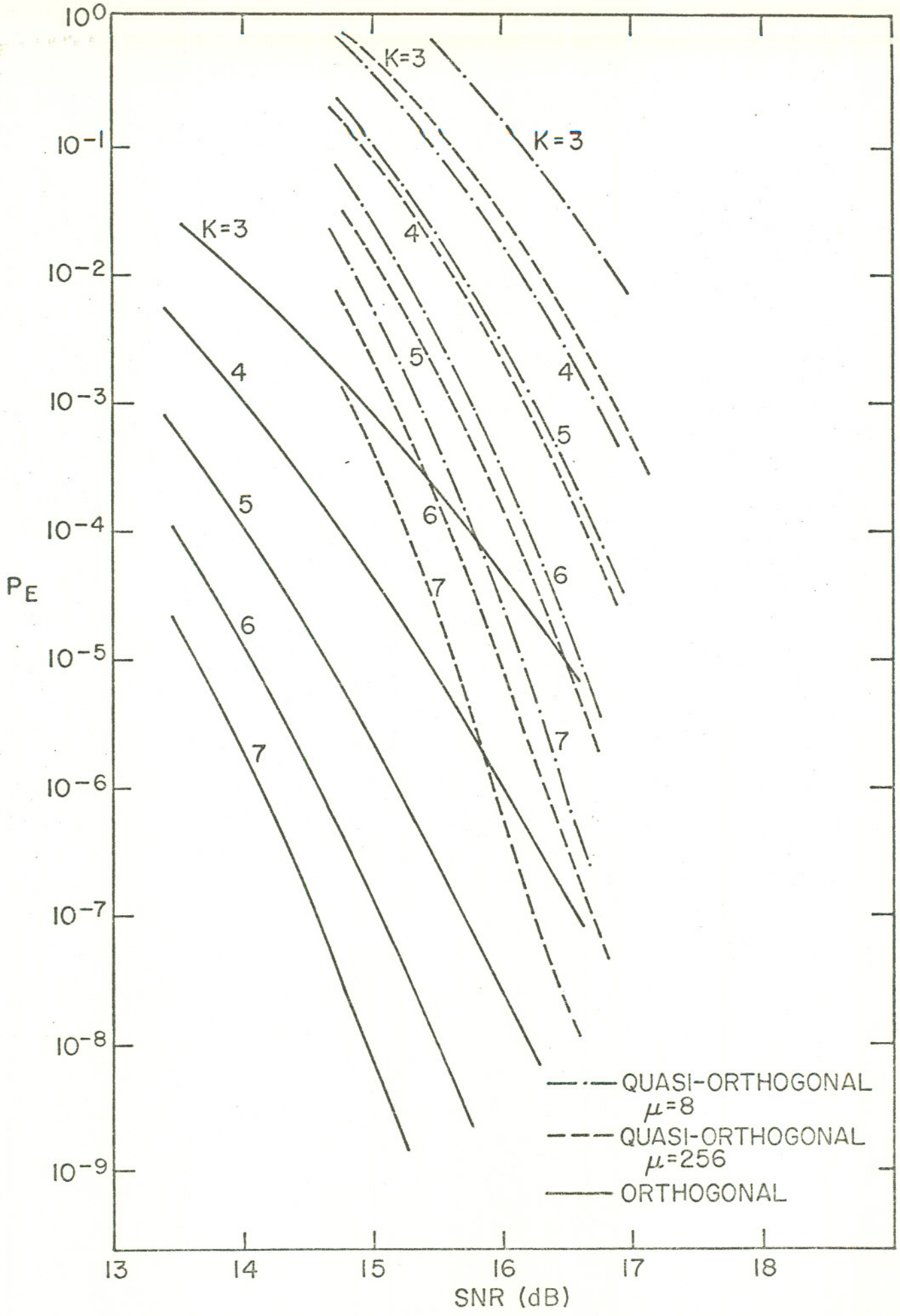

Fig. 8g. COMPARISON OF INCOHERENT ORTHOGONAL AND QUASI-ORTHOGONAL HARD QUANTIZING SCHEMES (L=200)

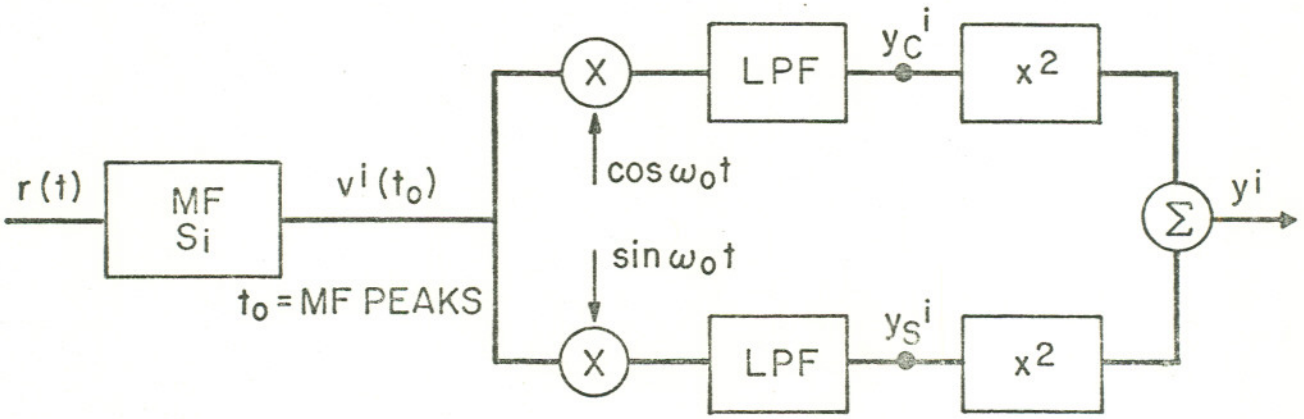

Fig. 9. EXPANDED VIEW OF CHANNEL "i" FOR INCOHERENT RECEIVER

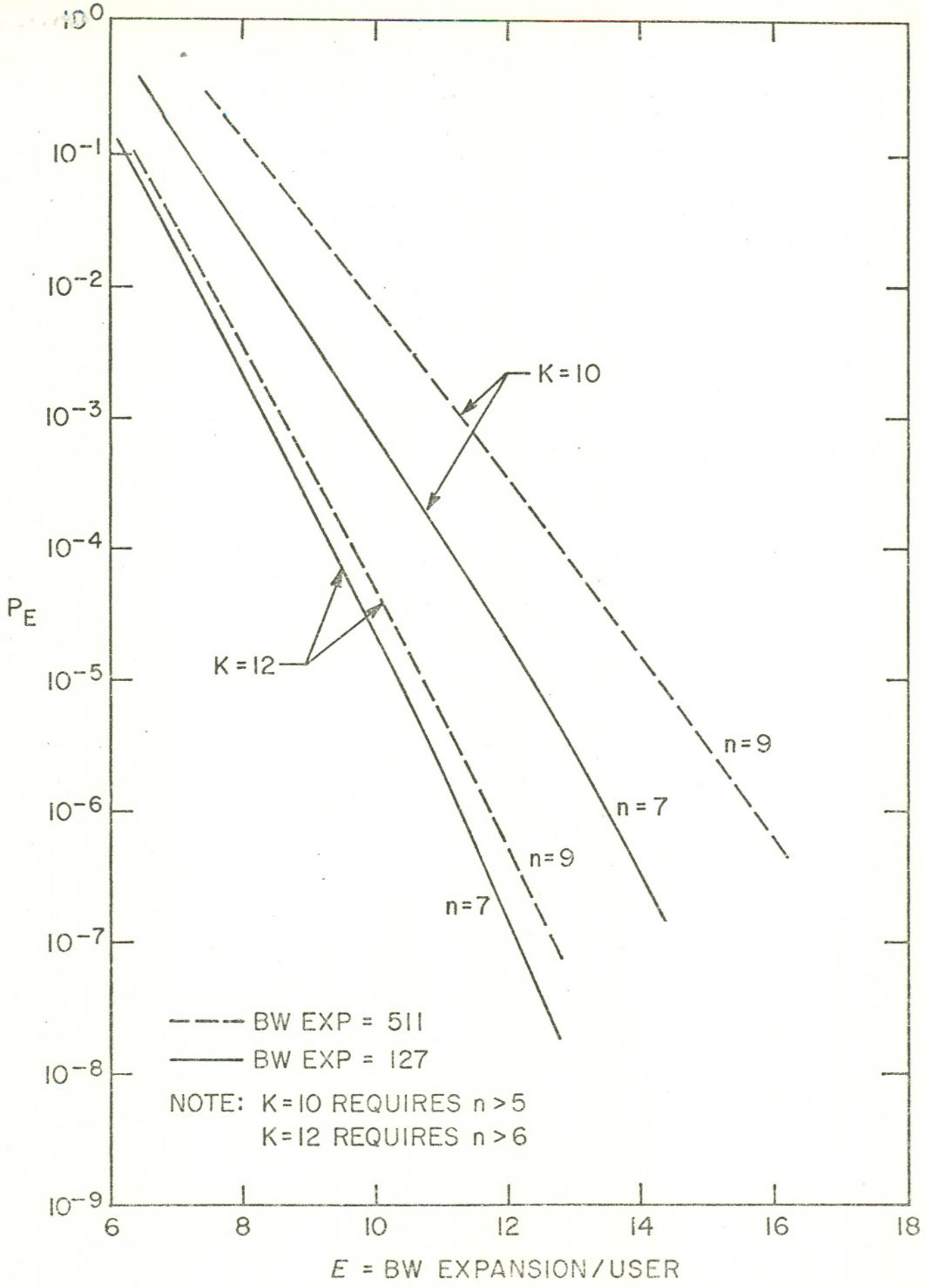

Fig. 10. MULTIPLE ACCESS WITH QUASI-ORTHOGONAL (GOLD CODES) TREE CODE (L=200)